PHYSICAL REVIEW B VOLUME 45, NUMBER 4 15 JANUARY 1992-II

Density-of-states effects in lateral-surface superlattices

J. Smoliner, V. Rosskopf, G. Berthold, E. Gornik, G. Böhm, and G. Weimann
Walter Schottky Institut, Technische Universität München, Am Coulombwall, D-8046 Garching, Germany
(Received 28 June 1991; revised manuscript received 9 September 1991)

We have investigated the transport properties of lateral-surface superlattices fabricated by laser holography on modulation-doped GaAs-$Al_xGa_{1-x}As$ field-effect transistors. Peaks in the differential drain-source resistance are observed in a range where the Fermi level has the same order of magnitude as the potential modulation. If a magnetic field is applied perpendicular to the sample, these peaks are shifted while the peak spacing is increased. Using a two-dimensional numerical model, we show that these effects are caused by a modulation density of states in the superlattice potential.

Lateral-surface superlattices (LSSL's) fabricated on high-mobility two-dimensional electron-gas systems are a topic of increased interest in the last few years. On field-effect transistors with grid-gate structure, transconductance oscillations are attributed to electron-backscattering effects[1,2] in the lateral-surface superlattice. A large negative differential resistance in the drain-source current was explained by the onset of Bloch oscillations[3] or sequential resonant tunneling processes between low-dimensional states beneath the gate contact.[4] On grating-gate field-effect transistors, which consist of many parallel quantum wires, even a modulation of the electron mobility was observed.[5] If an additional magnetic field is applied to such LSSL's, a number of magnetotransport effects can be studied. Both in weakly modulated grating[6] and square superlattice geometries[7] low field magnetoresistance oscillations are observed, which are equally spaced along the $1/B$ coordinate axis. Similar effects also occur in a hexagonal geometry superlattice generated by latex sphere etching masks.[8] In linearly modulated potentials, two sets of low field magnetoresistance oscillations were observed in a range where the Fermi energy is in the same order of magnitude than the potential modulation.[9] Due to a locally modulated density of states, electrons are transferred between regions of high and low mobility. This leads to resistance maxima, each time the electron concentration is high in low mobility areas and resistance minima, if electrons are transferred into areas of high mobility. In strongly modulated antidot-like superlattices, a large magnetoresistance peak was observed below 0.5 T and explained by reduced electron diffusion due to crystallization effects.[10] Further, this structure reflects the commensurability between the cyclotron diameter and the lattice period.[11] Most recently, even evidence of commensurate orbits impaled upon small groups of antidots was found.[12]

In this paper, we investigate the transport and magnetotransport properties of gated lateral-surface superlattices fabricated on modulation-doped GaAs-$Al_xGa_{1-x}As$ heterostructures. A series of peaks in the differential sample resistance is observed in a regime where the Fermi energy is in the same order of magnitude as the potential modulation. Using a two-dimensional numerical model, we demonstrate that this behavior is a consequence of an oscillatory density of states.

The samples consist of an unintentionally p-type doped GaAs layer grown on a semiinsulating substrate ($N_A < 10^{14}$ cm^{-3}), followed by an undoped spacer ($d = 120$ Å) with an aluminum concentration of 32%, and doped $Al_xGa_{1-x}As$ ($d = 400$ Å, $N_D = 2\times10^{18}$ cm^{-3}) The additional GaAs cap layer is highly n-type doped ($d = 150$ Å, $N_D = 3\times10^{18}$ cm^{-3}). At 4.2 K, we measured an electron concentration of 4.1×10^{11} cm^{-2} and a mobility of $\mu = 7\times10^5$ cm^2/Vs. Bar-shaped mesas were etched into the samples and Ohmic contacts were aligned using a Au-Ge alloy. A photoresist dot array having a period of $a = 400$ nm was fabricated on the mesas by laser holography. To induce a modulated electron density in the two-dimensional electron gas, the photoresist pattern was etched into the GaAs. After removing the photoresist, a Au gate was evaporated. A schematic view of a structured sample is shown in Fig. 1(a). Due to the surface tension of the wet chemical etchant, the etch grooves in the middle of the uncovered areas (cut 2) are deeper than directly between two neighbored photoresist dots (cut 1). Thus, the resulting potential is higher along cut 2 than along cut 1. A schematic view of the potential is given in Fig. 1(b). Cut 1 corresponds to a situation where $x = 200$ or 600 nm, cut 2 corresponds to $x = 0$ or 400 nm.

In Fig. 2 the measured sample resistance R_{DS} and its derivative dR_{DS}/dV_g are plotted versus gate voltage V_g. The measurements were carried out at a constant drain-source current of $I_{DS} = 2\times10^{-8}$ A and a temperature of $T = 1.8$ K. The derivatives were recorded by conventional modulation techniques using a modulation voltage of 0.1 mV and a modulation frequency of 131 Hz. In the considered gate voltage range, the R_{DS} curve shows a roughly exponential behavior. However, a set of oscillations is observed in the dR_{DS}/dV_g characteristics between $V_g = 0$ and 300 mV. At $B = 0$ T, the spacing between these peaks increases from $\Delta V_g = 24$ to 36 mV with more negative bias voltage. At $B = 0.5$ T, the distances between these peaks are larger and we observe eight with spacings between $\Delta V_g = 28$ and 50 mV. Note that the somewhat irregular shape of the measured peaks reflects

 ©1992 The American Physical Society

the onset of Shubnikov–de Haas oscillations.

Below $V_g=-380$ mV, the area beneath the gate contact is completely depleted, which is indicated by a constant drain-source resistance in the order of several MΩ independent of the applied gate voltage. Thus, the Fermi level is decreased from $E_F=14.3$ meV at $V_g=0$ V to $E_F=0$ meV at $V_g=-380$ mV, which means that the Fermi energy scales with gate voltage at a rate of $\Delta E_F/\Delta V_g=37$ meV/V. Therefore, the voltage spacings between the resistance maxima correspond to energy differences between 0.74 and 1.1 meV at $B=0$ T. At $B=0.5$ T, the energy spacings vary from 1.03 to 1.85 meV.

To explain the observed differential resistance oscillations, we start from the relation $R_{DS}=V_{DS}/(jw)$ with $j=evn$. j is the current density, w is the channel width, e is the electron charge, v is the electron drift velocity, and n the 2D electron concentration. The drift velocity is equal to $v=\mu V_{DS}/1_{DS}$, where 1_{DS} is the channel length. As the electron mobility does not change significantly in the considered gate voltage range, with $f(E)$ as Fermi distribution function, we express j as

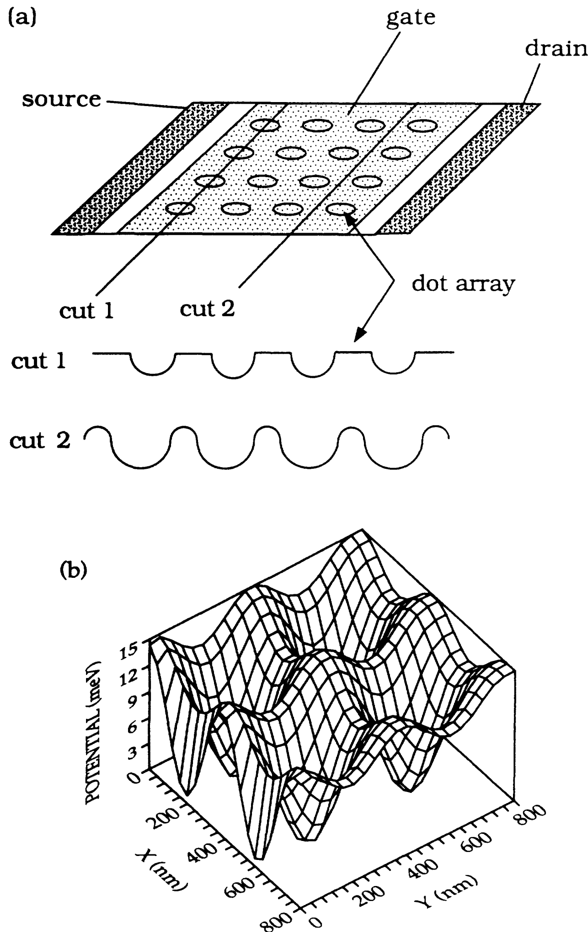

FIG. 1. (a) Schematic view of the sample. Cuts (1) and (2) illustrate the local variation of the etch profile. (b) Corresponding modulated potential in the two-dimensional electron gas.

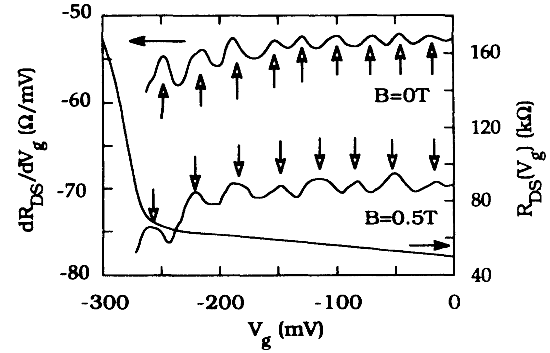

FIG. 2. R_{DS} vs V_g and dR_{DS}/dV_g vs V_g characteristics for $B=0$ and 0.5 T measured at 1.8 K. The arrows indicate the dR_{DS}/dV_g peak positions. The $B=0.5$ T curve is shifted to fit on the same plot.

$$j=ev\int D(E)f(E)dE \ . \tag{1}$$

Thus, the current density is directly related to the density of states $D(E)$ in the two-dimensional periodic potential $V(x,y)$.

Taking into account that the potential modulation along cut 2 is stronger than along cut 1 (see Fig. 1), we chose the following model potential:

$$V(x,y)=V_0[\cos(2\pi x/a)+\cos(2\pi y/a) -\tfrac{1}{2}\cos(2\pi x/a)\cos(2\pi y/a)+2.5]/4 \ . \tag{2}$$

A potential modulation of $V_0=15$ meV was deduced from the etch depth dependent electron densities measured on unstructured test samples. Deep in the potential ($E<6$ meV), the electrons are bound in quantized states. Above $E=6$ meV, an electron has enough energy to move through the valleys of the potential. This means that the potential shows antidotlike characteristics in this range. At even higher energies ($E>V_0$) an electron can move freely through the sample. If the Fermi level is swept through the potential, the electrons in the LSSL are tuned continuously from two-dimensional to zero-dimensional behavior. Thus, all structures in the density of states at $E=E_F$ are directly reflected in the R_{DS} versus V_g and dR_{DS}/dV_g characteristics. $D(E)$ is calculated as

$$D(E)=\frac{1}{(2\pi)^2}\int\frac{dL}{|\text{grad}\,[E(k_x,k_y)]|} \ . \tag{3}$$

In the two-dimensional case, the integration is carried out along lines of constant energy. To obtain the dispersion relations $E(k_x,k_y)$, the Schrödinger equation is solved numerically by finite-difference methods using the potential given in Eq. (2). The influence of small magnetic fields is also included into the model. More details of this method are published elsewhere.[13]

Using the assumption that the potential is not changed by the applied voltage, the results of this calculation are shown in Fig. 3. We first discuss the case of zero magnetic fields. At low energies ($E<6$ meV), the density of states shows a series of sharp peaks, which directly reflects the zero-dimensional states deep in the potential.

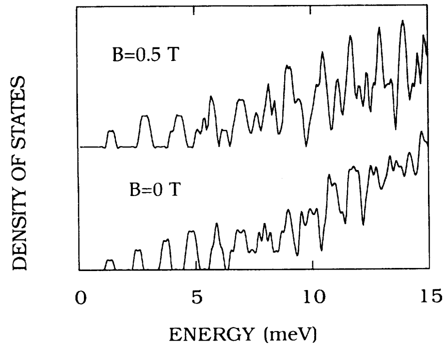

FIG. 3. Calculated density of states at $B=0$ and 0.5 T. The $B=0.5$ T curve is shifted to fit on the same plot.

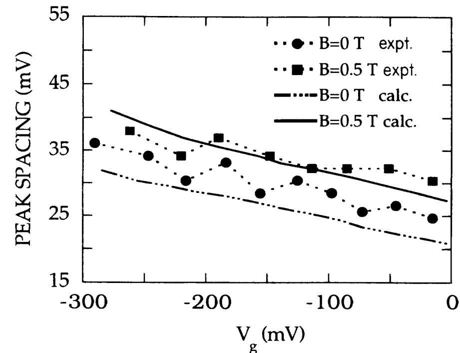

FIG. 4. Comparison between calculated and measured dR_{DS}/dV_g peak spacings at $B=0$ and 0.5 T.

The spacing between these 0D subbands is in the order of 1 meV. For increasing energies, the subband spacing becomes smaller because the potential becomes broader. Above $E=6$ meV, $D(E)$ starts to increase continuously, which means that now the electrons have enough energy to overcome the barriers in the modulated potential (e.g., along cut 1 in Fig. 1). Although the electrons are no longer bound in this energy range, the corresponding density of states still oscillates. In this regime, the subband spacing is much smaller than the distance between the density-of-states maxima. The large $D(E)$ oscillations are due to the varying degeneracy of LSSL subbands. The superimposed fine structure is explained by the occurrence of local $E(k_x,k_y)$ extrema in single energy bands. Near $E=15$ meV, both the amplitude and the period of the oscillations become smaller. In addition, the curve saturates, which indicates the transition to the usual $D(E)$=const behavior for unstructured two-dimensional electron-gas systems. Figure 3 also shows the result of a calculation carried out at $B=0.5$ T. Compared to the $B=0$ T curve, the spacings between the large structures in $D(E)$ are systematically increased. In addition, the amplitude of the $D(E)$ oscillation is larger and the superimposed fine structure is less pronounced, which reflects a more Landau-level-like behavior of the energy bands in the LSSL potential.

Since at 1.8 K, the energy differences between the fine-structure peaks are much smaller than kT, the fine structure in the density of states is not resolved in the present experiment. Thus, we only consider the distances between the large oscillations, which are plotted versus gate voltage in Fig. 4. If we further assume that the potential is not changed by the applied gate voltage, the calculated oscillatory behavior of $D(E)$ is well related to the properties of the measured dR_{DS}/dV_g characteristics. At $B=0$ T, the calculated peak distance decreases from $\Delta V_g^{\text{calc}}=33$ to 21 mV in the considered voltage range, which is in good agreement with the experimental data of $\Delta V_g^{\text{expt}}=36$ and 24 mV, respectively. The systematic deviations between the measured and calculated results are mainly due to the difference between the model potential and the real potential distribution in the LSSL. The fluctuations of the measured data might be explained by the fine structure in $D(E)$. To prove this quantitatively, however, the exact shape of the potential has to be known.

The agreement between theory and experiment is even better if a magnetic field is applied perpendicular to the plane of the modulated two-dimensional electron gas. In this case, the contribution of the magnetic field becomes comparable to V_m, so that the calculated results depend less on the exact choice of the electrostatic potential. At $B=0.5$ T, we obtain spacings of $\Delta V_g^{\text{calc}}=27$ mV at $V_g=0$ V and $\Delta V_g^{\text{calc}}=42$ mV at $V_g=-300$ mV, which agree well with the measured results of $\Delta V_g^{\text{expt}}=30$ mV ($V_g=0$ V) and $\Delta V_g^{\text{expt}}=38$ mV ($V_g=-300$ mV).

The steep increase of the dR_{DS}/dV_g curve around $V_g=-275$ mV is also understood within this model. Below $V_g=250$ mV, the Fermi level is tuned into a range ($E<6$ meV) where the electron energy is smaller than the potential modulation. In this range, all carriers are bound in 0D subbands and the transport properties are dominated by hopping or tunneling processes. Thus, the sample resistance is expected to increase.

It must be emphasized that such $D(E)$ oscillations occur in any type of periodic potential. Our simulations have shown that they are pronounced best in a sinusodial antidot-type superlattice. Here, a modulated density of states typically exists in an energy range between $E=0$ and $2V_0$. A large potential modulation at small grating period leads to a strongly modulated density of states, which in the ideal case results in several zones of negative differential resistance in the I_{DS} versus V_g characteristics.[4] Since in our sample we have a mixture between a dot-type and antidot-type LSSL and the grating periods is relatively large, the measured differential resistance peaks are rather weak.

If the magnetic field is varied and V_g is held constant, minima and maxima in the density of states will pass the Fermi energy. As the spacings between the density-of-states oscillations depend almost linearly on the magnetic field and further, the density of states peaks are roughly equidistant, magnetoresistance oscillations equally spaced along the $(1/B)$ coordinate axis will occur. In fact, such a behavior was reported for weakly modulated square and hexagonal superlattice geometries.[7,8] For similar reasons, magnetoresistance oscillations equally spaced in

$1/B$ are also observed in linearly modulated superlattices.[6] In strongly modulated potentials, however, these structures are washed out by other effects, causing single large peaks at low magnetic fields.[9,11,14]

In summary, the transport properties of lateral-surface superlattices were investigated in a regime where the Fermi energy is of the same order of magnitude as the potential modulation. Through a two-dimensional numerical model it was show that the observed peaks in the differential sample resistance are due to an oscillatory density of states. In weakly modulated potentials, these dR_{DS}/dV_g structures are equivalent to magnetoresistance oscillations, which are equally spaced in $1/B$.

ACKNOWLEDGMENTS

The authors are grateful to P. Vogl for helpful discussions. This work was sponsored by Deutsche Forschungsgemeinschaft, project no. Go469/4-1.

[1] K. Ismail, W. Chu, D. A. Antoniadis, and H. I. Smith, Appl. Phys. Lett. **52**, 1071 (1988).

[2] K. Ismail, W. Chu, D. A. Antoniadis, and H. I. Smith, J. Vac. Sci. Technol. B **6**, 1824 (1988).

[3] G. Bernstein and K. Ferry, J. Vac. Sci. Technol. B **5**, 964 (1987).

[4] K. Ismail, W. Chu, A. Yen, D. A. Antoniadis, and H. I. Smith, Appl. Phys. Lett. **54**, 460 (1989).

[5] K. Ismail, D. A. Antoniadis, and H. I. Smith, Appl. Phys. Lett. **54**, 1130 (1989).

[6] D. Weiss, K. v. Klitzing, K. Ploog, and G. Weimann, Europhys. Lett. **8**, 179 (1989).

[7] E. S. Alves, P. H. Beton, M. Henini, L. Eaves, P. Main, O. H. Huges, G. A. Toombs, S. P. Beaumont, and C. C. W. Wilkinson, J. Phys. C **1**, 8257 (1989).

[8] H. Fang and P. J. Stiles, Phys. Rev. B **41**, 10 171 (1990).

[9] G. Berthold, J. Smoliner, W. Demmerle, F. Hirler, E. Gornik, G. Böhm, and G. Weimann, Semicond. Sci. Technol. **6**, 709 (1991).

[10] A. Lorke, J. P. Kotthaus, and K. Ploog, Phys. Rev. B **44**, 3447 (1991).

[11] K. Ensslin and P. M. Petroff, Phys. Rev. B **41**, 12 307 (1990).

[12] D. Weiss, M. L. Roukes, A. Menschig, P. Grambow, K. v. Klitzing, and G. Weimann, Phys. Rev. Lett. **66**, 2790 (1991).

[13] J. Smoliner, G. Berthold, and N. Reihnacher, Semicond. Sci. Technol. **6**, 642 (1991).

[14] P.H. Beton, E. S. Alves, P. C. Main, L. Eaves, M. W. Dellow, M. Henini, O. H. Huges, S. P. Beaumont, and C. D. W. Wilkinson, Phys. Rev. B **42**, 9229 (1990).